Pyridyl-Amides as a Multimode Self-Assembly Driver for the Design of a Stimuli-Responsive π-Gelator

ARTICLE *in* CHEMISTRY - AN ASIAN JOURNAL · APRIL 2015

Impact Factor: 4.59 · DOI: 10.1002/asia.201500331 · Source: PubMed

ACES
DOI: 10.1002/asia.201500331
CHEMISTRY
AN ASIAN JOURNAL
Full Paper

Self-Assembly

Pyridyl-Amides as a Multimode Self-Assembly Driver for the Design of a Stimuli-Responsive π-Gelator

Kalathil K. Kartha,[a] Vakayil K. Praveen,[a] Sukumaran Santhosh Babu,[a] Sandeep Cherumukkil,[a, b] and Ayyappanpillai Ajayaghosh*[a, b]

Abstract: An oligo(*p*-phenylenevinylene) (OPV) derivative connected to pyridyl end groups through an amide linkage (**OPV-Py**) resulted in a multistimuli-responsive π-gelator. When compared to the corresponding OPV π-gelator terminated by a phenyl-amide (**OPV-Ph**), the aggregation properties of **OPV-Py** were found to be significantly different, leading to multistimuli gelation and other morphological properties. The pyridyl moiety in **OPV-Py** initially interferes with the amide H-bonded assembly and gelation, however, protonation of the pyridyl moiety with trifluoroacetic acid (TFA) facilitated the formation of amide H-bonded assembly leading to gelation, which is reversible by the addition of *N,N*-diisopropyethylamine (DiPEA). Interestingly, addition of Ag^+ ions to a solution of **OPV-Py** facilitated the formation of a metallo-supramolecular assembly leading to gelation. Surprisingly, ultrasound-induced gelation was observed when **OPV-Py** was mixed with a dicarboxylic acid ($\mathbf{A_1}$). A detailed study using different spectroscopic and microscopic experimental techniques revealed the difference in the mode of assembly in the two molecules and the multistimuli-responsive nature of the **OPV-Py** gelation.

Introduction

π-Gels are an intriguing class of soft materials created through the self-assembly of π-systems.[1] Research on these materials has been intensively pursued by virtue of their interesting optoelectronic properties useful for applications in organic electronics and photonics.[1–3] In many of the cases, self-assembly of π-systems results in the formation of extended superstructures that leads to the gelation of solvents depending on factors such as structure of molecules, solvent polarity, temperature, and concentration.[1–4] Recent studies have revealed that to attain a desired molecular organization and gel formation, control over self-assembly and its nucleation-elongation pathways are important.[5,6] Nucleation followed by elongation through extended amide H-bonding and π-stacking resulting in the formation of one-dimensional (1-D) fibers is a good way of controlling the molecular assembly and gel formation.[6,7]

Several amide-functionalized self-assembling systems and gelators containing ferrocene, tetrathiafulvalene, thiophene, pyridine, etc. are known to respond to various external stimuli such as redox reagents, metal ions, acids, and ultrasound.[7,8] In such cases, favorable and/or preferred aggregation pathways can be triggered by the introduction of a second component.[8] For this purpose, pyridine is a preferred moiety, which is known to interact with different metal ions and acids.[9–11] Even though a number of assemblies and gels based on pyridine-functionalized systems are known, a clear understanding of the role of pyridyl amide on the aggregation and gelation properties of π-systems is lacking.

We have reported a number of functionalized OPVs and their gelation from nonpolar hydrocarbon solvents at extremely low concentrations.[12–14] Through a series of experiments, the role of functional groups in OPVs and the role of solvents in the gelation process have been revealed.[12–14] Our success with OPV-based π-gelators have encouraged several research groups to modify OPV backbones with different functionalities.[15] Herein, we demonstrate that the integration of a pyridyl nitrogen as an additional noncovalent interacting position in the OPV gelator (**OPV-Ph**) results in a dramatic change in the self-assembly and gelation behavior, leading to a new multistimuli-responsive π-gelator (**OPV-Py**).

[a] *Dr. K. K. Kartha, Dr. V. K. Praveen, Dr. S. S. Babu, S. Cherumukkil, Prof. Dr. A. Ajayaghosh*
Photosciences and Photonics Group, Chemical Sciences and Technology Division
CSIR-National Institute for Interdisciplinary Science and Technology (CSIR-NIIST)
Trivandrum 695 019, Kerala (India)
E-mail: ajayaghosh@niist.res.in

[b] *S. Cherumukkil, Prof. Dr. A. Ajayaghosh*
Academy of Scientific and Innovative Research (AcSIR)
CSIR-National Institute for Interdisciplinary Science and Technology (CSIR-NIIST)
Trivandrum 695 019, Kerala (India)

Supporting information for this article is available on the WWW under http://dx.doi.org/10.1002/asia.201500331.

Results and Discussion

The phenyl-amide functionalized gelator, **OPV-Ph** and the pyridyl-amide functionalized OPV derivative, **OPV-Py** (Figure 1), were synthesized as depicted in Scheme S1 in the Supporting Information. For this purpose, the OPV-bisester (**OPV2**) was synthesized using a Wittig–Horner reaction of the phosphonate ester of ethyl 2-bromoacetate with the OPV-bisaldehyde (**OPV1**), which was prepared according to a known procedure.[12b,16] Hydrolysis of **OPV2** using KOH in methanol yielded **OPV3**. The final reaction between **OPV3** and the amine derivative was conducted using 1[bis(dimethylamino)methylene]-1*H*-1,2,3-triazolo[4,5-*b*]pyridinium 3-oxid hexafluorophosphate (HATU) in the presence of DiPEA. All these compounds were characterized using FT-IR, ^{1}H NMR, and ^{13}C NMR spectroscopies and MALDI-TOF mass spectrometry.

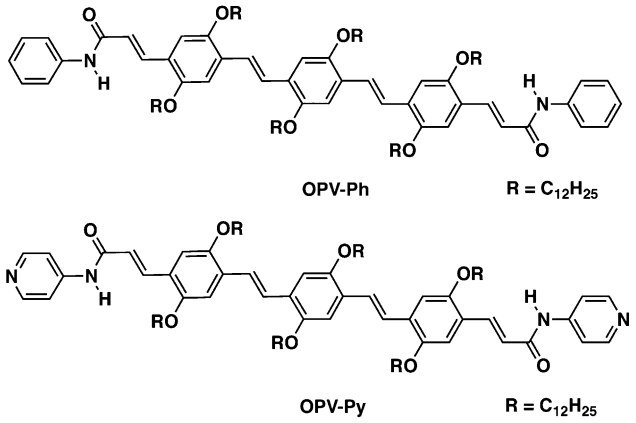

Figure 1. Molecular structures of phenyl-amide and pyridyl-amide functionalized OPV derivatives.

Variable-temperature absorption spectral changes of **OPV-Ph** and **OPV-Py** in toluene (5×10^{-5} M) exhibited a distinct behavior as shown in Figure 2. **OPV-Ph** in toluene at 70 °C showed an absorption maximum at 445 nm, corresponding to the monomeric species. At 20 °C, a blue-shifted absorption band at $\lambda_{max}=420$ nm ($\Delta\lambda=1338$ cm^{-1}) with a small vibronic shoulder band at 518 nm was observed (Figure 2a). Similarly, a decrease in temperature resulted in quenching of the fluorescence intensity due to the formation of **OPV-Ph** aggregates (Figure S1a in the Supporting Information). Contrary to the behavior of **OPV-Ph**, no considerable shift in the absorption maximum was noted for **OPV-Py** with an increase in temperature in toluene (Figure 2b). However, a strong red-shifted vibronic shoulder band at 520 nm was observed with relatively less decrease in the intensity of the π–π^* transition band at 448 nm. The emission of **OPV-Py** aggregates in toluene at 20 °C exhibited a shift to lower wavelengths with an increase in intensity at higher temperatures, indicating the breaking of the self-assembly (Figure S1b in the Supporting Information). In addition, we found that **OPV-Py** in $CHCl_3$ (5×10^{-5} M; Figure S2 in the Supporting Information) has the tendency to form aggregates, whereas **OPV-Ph** was found to be highly soluble and exists as the monomeric species (Figure S3 in the Supporting Information).

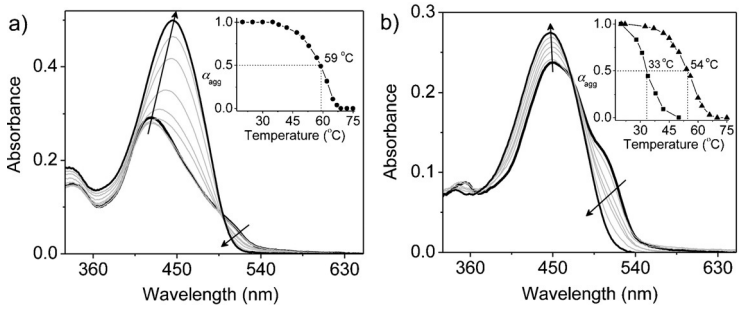

Figure 2. Variable-temperature absorption changes of (a) **OPV-Ph** and (b) **OPV-Py** in toluene (5×10^{-5} M). Arrows indicates relative changes in absorption with increase in temperature from 20 to 70 °C. Insets show plots of fraction of aggregate (α_{agg}) vs. temperature. Figure 2a inset: **OPV-Ph** in toluene (●). Figure 2b inset: **OPV-Py** in toluene (▲) and chloroform (■).

The stability of the aggregates was determined from the plot of the fraction of aggregate (α_{agg}) versus temperature (Figure 2 insets). A melting transition temperature (T_m, temperature at which $\alpha_{agg}=0.50$) of 59 °C was obtained for **OPV-Ph** in toluene, whereas **OPV-Py** aggregates showed a T_m of 54 and 33 °C in toluene and chloroform, respectively. These observations suggest that the aggregation modes of **OPV-Ph** and **OPV-Py** are significantly different from each other, which emphasize the importance of the terminal functional moiety in the amide linkage in controlling the aggregation properties. Having seen a difference in the aggregation modes of the two molecules, we further examined their gel formation in toluene. As expected, **OPV-Ph** formed a gel in toluene at a critical gelator concentration (CGC) of 0.45 mM (Figure S4 in the Supporting Information). Surprisingly, **OPV-Py** did not form a gel, even at higher concentrations, underlining that the difference in the mode of aggregation has a significant influence on the gelation behavior.

The above observations indicate that **OPV-Ph** preferably forms an H-type assembly through the amide H-bonding (Figure 3a), whereas **OPV-Py** likely forms a random assembly (Figure 3b). Formation of such non-gelling random assembly can be explained by the interference of the terminal pyridyl moiety with the amide H-bonding in **OPV-Py**. If so, protonation of the pyridyl moiety should facilitate the aggregation of the **OPV-Py** through amide H-bonding, leading to the gelation of the solvent. As hypothesized, addition of 1 equivalent of TFA to the solution of **OPV-Py** in $CHCl_3$ (5×10^{-5} M) resulted in a red-shift in the absorption maximum from 448 to 474 nm with a slight decrease in the intensity (Figure 4a). In addition, the emission was significantly quenched and became broad with loss of vibronic features (Figure 4a inset). Addition of 2 equivalents of TFA induced a further shift of the absorption maximum to 492 nm and the emission maximum to 610 nm (Figure 4a). These changes in absorption and emission wavelengths are also visible in the photographs (Figure S5a and S5b in the Supporting Information) of the $CHCl_3$ solutions of **OPV-Py** before (greenish-yellow color) and after

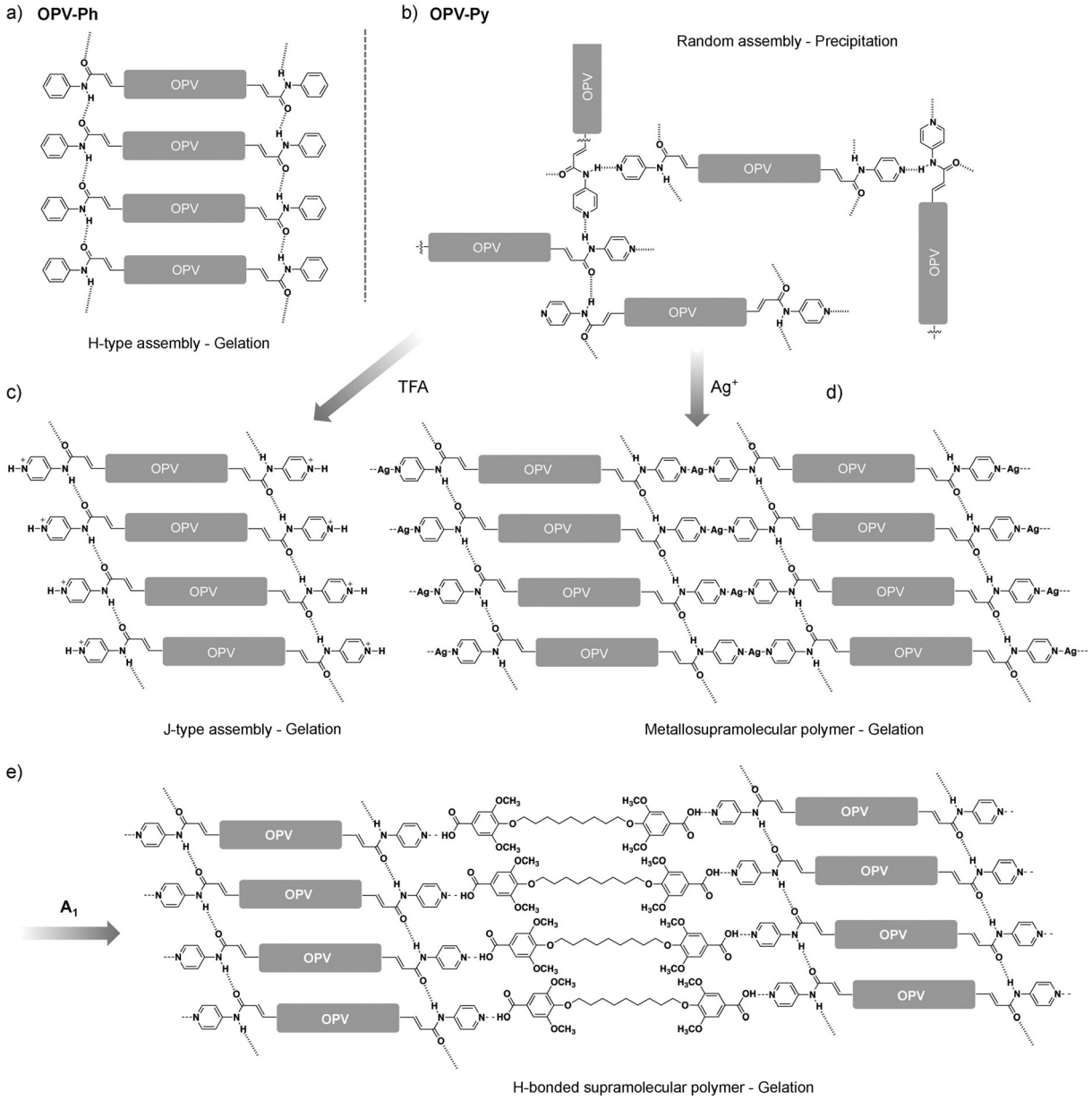

Figure 3. Schematic representation of the self-assembling mode of (a) **OPV-Ph** and (b) **OPV-Py**, and the stimuli-responsive self-assembly of **OPV-Py** in the presence of (c) TFA, (d) Ag^+, and (e) the aromatic dicarboxylic acid $\mathbf{A_1}$.

the addition of TFA (orange-red color). Obviously, these spectral shifts of **OPV-Py** with TFA are different from the blue-shift in the absorption spectrum of **OPV-Ph**, indicating that the mode of assembly in both molecules is different. While in the latter case an H-type assembly (Figure 3a) is evident, the former case points towards a J-type assembly (Figure 3c). Further evidence for aggregation of **OPV-Py** in the presence of TFA is obtained from the ^{1}H NMR spectrum, which exhibited a broadening of peaks upon addition of TFA (Figure S5c in the Supporting Information). The red-shift in the absorption and emission spectra as well as broadening of ^{1}H NMR signals indicate the formation of extended hierarchical assemblies of **OPV-Py** in the presence of TFA and are further revealed from morphological studies (see below). Addition of TFA to a solution of **OPV-Ph** in $CHCl_3$ (5×10^{-5} M) did not show any considerable changes in the absorption and emission spectra (Figure S6 in the Supporting Information), which point towards the importance of the pyridine heteroatom in the **OPV-Py** for inducing a stimuli-responsive character.

Upon increasing the temperature from 25 to 50 °C, **OPV-Py** in $CHCl_3$ in the presence of 2 equivalents of TFA (Figure 4b) displayed a blue-shift ($\Delta\lambda = 963$ cm^{-1}) in the absorption maximum without much change in the intensity, and the fluorescence profile showed a slight increase in the intensity. The decrease in the absorbance at 560 nm with increasing temperature must be due to the breaking of the protonated **OPV-Py** aggregates. Addition of 2.2 equivalents of organic base (DiPEA) to **OPV-Py**-TFA aggregates resulted in the formation of mono-

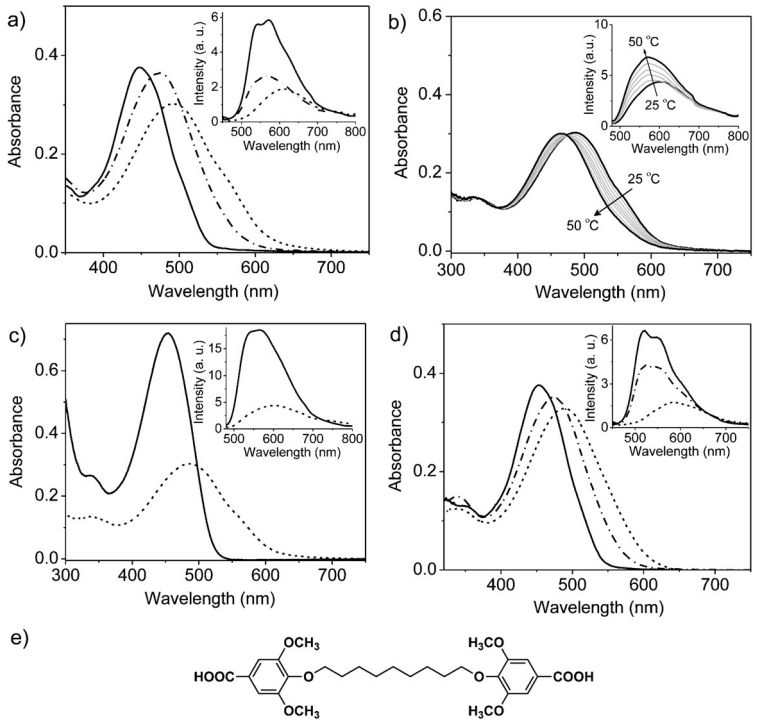

Figure 4. (a) Absorption spectra of **OPV-Py** in $CHCl_3$ containing 0 (——), 1 (–•–•), and 2 (-----) equiv. of TFA. (b) Variable-temperature absorption spectra of **OPV-Py** in $CHCl_3$ containing 2 equiv. of TFA. (c) Absorption spectra of **OPV-Py**-TFA before (-----) and after (——) addition of 2.2 equiv. of DiPEA. (d) Absorption spectra of **OPV-Py** in chloroform (containing 0 (——), 0.5 (–•–•) and 1 (-----) equiv. of AgOTf. Insets show the corresponding emission spectra. The concentration of **OPV-Py** was 5×10^{-5} M in all experiments. (e) Molecular structure of the dicarboxylic acid derivative $\mathbf{A_1}$.

mers as evident from the absorption and emission spectral shift owing to deprotonation followed by the complete disassembly of the **OPV-Py** (Figure 4c).

With these results in hand, we attempted the preparation of H-bonded supramolecular polymers of **OPV-Py** with an appropriate carboxylic acid. We have chosen a few organic acids for this purpose as shown in Chart S1 in the Supporting Information. Refluxing **OPV-Py** with the appropriate acid in a 1:1 stoichiometry in THF for 2 h at 60 °C followed by the removal of the solvent afforded the H-bonded complexes. Among the different acids tested, 4,4′-(nonane-1,9-diylbis(oxy))bis(3,5-dimethoxybenzoic acid), $\mathbf{A_1}$ (Figure 4e), gave the best results. At higher concentrations, the **OPV-Py**-$\mathbf{A_1}$ complex in $CHCl_3$ resulted in a stable gel upon heating and cooling, whereas precipitation occurred in toluene. Surprisingly, the precipitates of the **OPV-Py**-$\mathbf{A_1}$ complex formed a weak gel in toluene upon application of ultrasound (0.23 W cm^{-2}, 37 kHz) for 2 min. The sonication-induced gelation is most likely due to re-organization of the noncovalent interactions, as commonly observed in the case of ultrasound-induced gelation of H-bonded systems.[17]

Finally, we tried to modulate the aggregation properties of **OPV-Py** with Ag^+, which is known to coordinate with a pyridine moiety.[9] We titrated a solution of **OPV-Py** in $CHCl_3$ (5×10^{-5} M) with silver triflate (AgOTf). Electronic absorption and fluorescence spectral studies revealed that absorption and fluorescence intensities were decreased with an increase in the concentration of Ag^+ ions (Figure 4d). At 1:1 molar ratio, the absorption and emission maxima were red-shifted with a further decrease in the intensity. Upon increasing the concentration of **OPV-Py**, a stable gel in $CHCl_3$ was obtained in the presence of Ag^+ ions. This observation can be attributed to the formation of an extended linear metallosupramolecular polymer in solution (Figure 3d), the growth of which may be assisted by amide H-bonding and π-stacking.

The overall multistimuli-responsive behavior of **OPV-Py** is summarized in Figure 5. Upon addition of different external agents, like TFA, $\mathbf{A_1}$, and Ag^+, to a required concentration of **OPV-Py** in $CHCl_3$, gelation was observed after heating followed by cooling. Subsequently, a two-component gel[18] was derived from a hot toluene solution of **OPV-Py**-$\mathbf{A_1}$ upon sonication for 2 min. The critical gelator concentration (CGC) and gel melting temperature (T_{gel}) were determined by the 'inversion tube method' and the 'dropping ball method', respectively.[12] The results are summarized in Tables S1 and S2 in the Supporting Information. The CGC of the **OPV-Ph** toluene gel is 0.45 mM, a value lower than those of the **OPV-Py**-Ag^+ gel in $CHCl_3$ (2.83 mM), **OPV-Py**-TFA gel in $CHCl_3$ (2.92 mM), **OPV-Py**-$\mathbf{A_1}$ gel in $CHCl_3$ (3.27 mM), and the sonication-induced gel in toluene (3.15 mM). Gel melting temperature studies showed a regular increase in gel stability with increasing concentration (Figure S7 in the Supporting Information). At a particular concentration, **OPV-Py**-TFA and **OPV-Py**-Ag^+ gels in $CHCl_3$ exhibited a maximum stability in comparison to **OPV-Py**-$\mathbf{A_1}$ $CHCl_3$ and toluene gels.

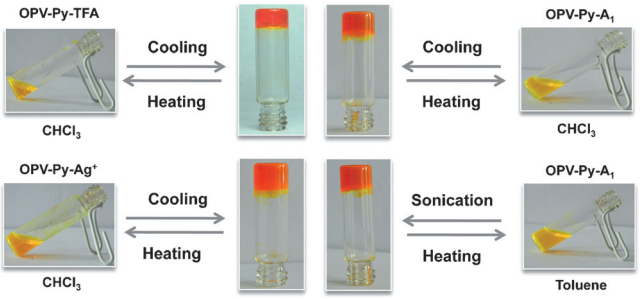

Figure 5. Multimode gelation of two-component systems based on **OPV-Py**.

Morphological features of **OPV-Py** assemblies prepared from toluene and $CHCl_3$ (5×10^{-5} M) were examined by atomic force microscopy (AFM) and transmission electron microscopy (TEM). Formation of short fiber bundles of 1–3 μm in length, 100–400 nm in width, and 50–300 nm in height were observed for the assemblies from toluene (Figure 6a and Figure S8a in the Supporting Information). However, the morphological feature of the assemblies obtained from $CHCl_3$ was different from those obtained from toluene. In this case, AFM images displayed short rods of 1–3 μm in length, 50–250 nm in width,

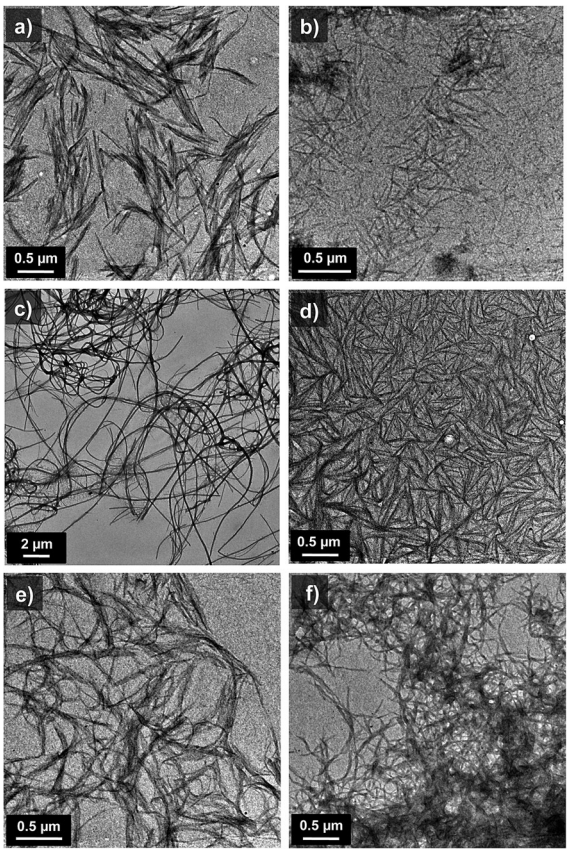

Figure 6. TEM images of OPV-amide aggregates (5×10^{-5} M). (a) **OPV-Py** in toluene, (b) **OPV-Py** in $CHCl_3$, (c) **OPV-Ph** in toluene, (d) **OPV-Py**-TFA in $CHCl_3$, (e) **OPV-Py**-Ag^+ in $CHCl_3$, and (f) **OPV-Py**-$\mathbf{A_1}$ in $CHCl_3$.

and 2-10 nm in height (Figure S8b in the Supporting Information), which was also confirmed by TEM studies (Figure 6b). However, in the case of **OPV-Ph**, samples prepared from a toluene solution (5×10^{-5} M) showed the presence of an extended fibrillar morphology having several micrometers in length, 100–300 nm in width, and 6–12 nm in height, as shown in Figure 6c and Figure S8c in the Supporting Information.

Contrary to the formation of needle-like short fibers in toluene, **OPV-Py** in the presence of TFA resulted in long flexible fibers of micrometers in length, 100–300 nm in width, and 5-30 nm in height (Figure 6d and Figure S9a in the Supporting Information). Similarly, a 1:1 complex of **OPV-Py** and Ag^+ ions in $CHCl_3$ (5×10^{-5} M) showed the presence of interconnected fibrous structures of a few micrometers in length, 100–300 nm in width, and 6–24 nm in height that are densely packed in large areas (Figure 6e and Figure S9b in the Supporting Information). Similar observations were made for aggregates of **OPV-Py**-$\mathbf{A_1}$ in $CHCl_3$ (5×10^{-5} M) as shown in Figure 6f and Figure S9c in the Supporting Information. **OPV-Py**-$\mathbf{A_1}$ assemblies from toluene are composed of ill-defined aggregates as well as fibers (Figure 7a). Upon sonication for 2 min, entangled fibers with a width of 50–250 nm, height of 10–50 nm, and several micrometers in length were observed as shown in Figure 7b. This is further confirmed through TEM analysis (Figure S10 in the Supporting Information).

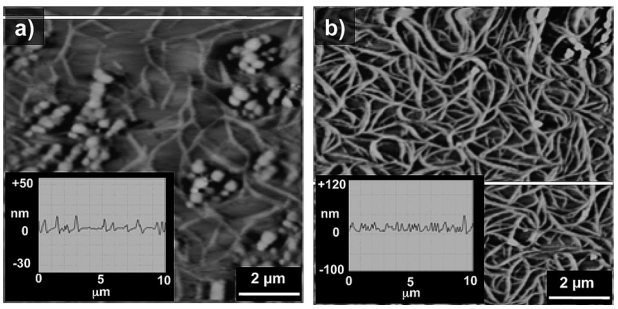

Figure 7. AFM images of **OPV-Py**-$\mathbf{A_1}$ aggregates in toluene (5×10^{-5} M) (a) before and (b) after sonication for 2 min. Insets show the corresponding cross-section analysis.

The packing of the molecules in the self-assembled state was investigated using FT-IR spectroscopy and X-ray diffraction (XRD) techniques. The xerogel film of **OPV-Ph** in toluene showed IR absorptions corresponding to H-bonded secondary amides such as ν_{N-H} at 3267 cm^{-1} (amide A band) and $\nu_{C=O}$ at 1657 cm^{-1} (amide I band) (Figure S11a in the Supporting Information).[6b,19] Similarly, in the case of **OPV-Py**-TFA and **OPV-Py**-Ag^+, the amide A and amide I bands were observed at 3263 and 1663 and at 3262 and 1666 cm^{-1}, respectively (Figure S11b, c in the Supporting Information), whereas the film state IR spectrum of **OPV-Py** aggregates in toluene displayed a broad ν_{N-H} band in the 3100–3600 cm^{-1} region due to multiple-type H-bonding (Figure S12 in the Supporting Information). The XRD pattern of the **OPV-Ph** xerogel prepared from toluene exhibited several well-defined peaks in the small- and wide-angle region, which suggests long-range ordering of the molecules (Figure S13a in the Supporting Information). The XRD peaks with *d*-values of 4.67 and 3.76 Å found in the wide-angle region can be ascribed to secondary amide H-bonding assisted 1-D-stacking of the molecules.[6b,19,20] Comparable observations were made in the XRD pattern of the **OPV-Py**-TFA and **OPV-Py**-Ag^+ xerogel films prepared from $CHCl_3$, which showed peaks with *d*-spacings of 4.43 and 3.75 Å and of 4.46 and 3.79 Å, respectively (Figure S13b and S13c in the Supporting Information). In all the cases, a prominent diffraction signal with a *d*-spacing value of around 27 Å was observed in the small-angle region, which is close to the calculated length between the two terminal amide units of OPV-amides (26.12 Å).

The effect of sonication on gelation was monitored with FT-IR and XRD studies as shown in Figure S14 and S15, respectively, in the Supporting Information. The IR spectrum of the **OPV-Py**-$\mathbf{A_1}$ complex showed absorption peaks at 3314 cm^{-1} for amide A band, 1690 cm^{-1} for $\nu_{C=O}$ acid, and 1663 cm^{-1} for amide I band. In the IR spectrum of the aggregates of **OPV-Py**-$\mathbf{A_1}$ in toluene, these peaks showed a shift towards a higher wavenumber such as 3441 cm^{-1} (broad) for amide A, 1722 cm^{-1} for $\nu_{C=O}$ acid, and 1693 cm^{-1} for amide I. Upon sonication, these peaks were shifted back to 3331, 1691, and 1665 cm^{-1}, respectively. As mentioned earlier, the aggregates of the **OPV-Py**-$\mathbf{A_1}$ complex precipitate out from the solution due to the formation of ill-defined aggregates. Upon sonication, the shift of the IR peaks to a lower wavenumber indicates

the formation of an H-bonded assembly through acid–pyridine interaction along with amide H-bonding. This is also supported by XRD studies (Figure S15 in the Supporting Information). The XRD profile of **OPV-Py-A_1** aggregates from toluene showed a broad peak in the wide-angle region. By contrast, after sonication, two distinct peaks were observed with a *d*-spacing of 4.45 and 3.72 Å as in the case of the XRD patterns of the **OPV-Py-A_1** xerogel in $CHCl_3$, which showed peaks with *d*-values of 4.43 and 3.71 Å in the wide-angle region. This observation indicates that the **OPV-Py-A_1** complex in $CHCl_3$ self-organizes in a well-defined manner when compared to that in toluene. Under ultrasound energy, breaking of the ill-defined aggregates by the reorganization of the noncovalent interactions might have resulted in the formation of kinetically trapped aggregates, leading to the nucleation of extended fibers that are responsible for the gel formation.

The observed difference in the self-assembly and gelation properties of the two molecules can be rationalized as shown in Figure 3. **OPV-Ph** forms the usual 1-D self-assembly through the amide H-bonding and π-stacking, resulting in gel formation in toluene. Such an assembly is hindered by the pyridyl moiety in **OPV-Py** through the involvement of the H-bonding between the amide H-atom and the pyridyl N-atom, leading to random supramolecular polymerization. This can be prevented by the protonation of the pyridyl moiety with TFA, triggering the interamide H-bonding self-assembly and gelation, which is reversible by deprotonation with DiPEA. Upon complexation with Ag^+, **OPV-Py** formed a metallo-supramolecular gel through extended metal-ion coordination, amide H-bonding, and π-stacking. Interaction of **OPV-Py** with an aromatic dicarboxylic acid (**A_1**) resulted in the formation of aggregates, which formed gels upon heating and cooling or upon sonication.

Conclusions

In conclusion, we have designed and synthesized two amide-functionalized OPV derivatives, **OPV-Ph** and **OPV-Py**, that contain benzene and pyridine, respectively, as the terminal substituents. **OPV-Ph** forms H-type aggregates and a gel in toluene. **OPV-Py** alone does not result in gelation in common nonpolar solvents; rather, it forms self-assembled precipitates. Gelation is realized by preparing two-component systems through the co-assembly of **OPV-Py** with an appropriate noncovalent partner. The protonation of **OPV-Py** with TFA facilitated the formation of H-bonding-directed J-type assembly, which was reversible by the addition of an organic base (DiPEA). **OPV-Py** formed extended metallo-supramolecular assemblies with Ag^+ ions, thereby leading to gel formation. Application of ultrasound facilitated the gel formation by the **OPV-Py-A_1** complex in toluene. The present system is a unique example to demonstrate how the presence of an additional noncovalent interaction site in a molecule generates the option for different self-assembly modes by multistimuli-responsive processes.

Acknowledgements

A.A. is grateful to the Department of Atomic Energy, Government of India, for a DAE-SRC Outstanding Researcher Award and for financial support of this work. K.K.K. and S.C. thank the Council of Scientific and Industrial Research (CSIR) and University Grants Commission (UGC), Government of India, respectively for research fellowships. We thank Mr. Kiran Mohan of CSIR-NIIST for TEM analyses.

Keywords: gels · H-bonding · multistimuli · oligo(*p*-phenylenevinylene)s · self-assembly

[1] a) S. S. Babu, V. K. Praveen, A. Ajayaghosh, *Chem. Rev.* **2014**, *114*, 1973–2129; b) S. S. Babu, S. Prasanthkumar, A. Ajayaghosh, *Angew. Chem. Int. Ed.* **2012**, *51*, 1766–1776; *Angew. Chem.* **2012**, *124*, 1800–1810; c) S. S. Babu, K. K. Kartha, A. Ajayaghosh, *J. Phys. Chem. Lett.* **2010**, *1*, 3413–3424; d) A. Ajayaghosh, V. K. Praveen, C. Vijayakumar, *Chem. Soc. Rev.* **2008**, *37*, 109–122.

[2] a) F. J. M. Hoeben, P. Jonkheijm, E. W. Meijer, A. P. H. J. Schenning, *Chem. Rev.* **2005**, *105*, 1491–1546; b) A. P. H. J. Schenning, E. W. Meijer, *Chem. Commun.* **2005**, 3245–3258; c) F. Würthner, T. E. Kaiser, C. R. Saha-Möller, *Angew. Chem. Int. Ed.* **2011**, *50*, 3376–3410; *Angew. Chem.* **2011**, *123*, 3436–3473; d) Y. Yamamoto, *Sci. Technol. Adv. Mater.* **2012**, *13*, 033001; e) E. Moulin, J. J. Cid, N. Giuseppone, *Adv. Mater.* **2013**, *25*, 477–487; f) S. Yagai, *Bull. Chem. Soc. Jpn.* **2015**, *88*, 28–58; g) A. Jain, S. J. George, *Mater. Today* **2015**, *18*, 206–214.

[3] a) B.-K. An, J. Gierschner, S. Y. Park, *Acc. Chem. Res.* **2012**, *45*, 544–554; b) L. Maggini, D. Bonifazi, *Chem. Soc. Rev.* **2012**, *41*, 211–241; c) Y. Yan, C. Zhang, J. Yao, Y. S. Zhao, *Adv. Mater.* **2013**, *25*, 3627–3638; d) V. K. Praveen, C. Ranjith, N. Armaroli, *Angew. Chem. Int. Ed.* **2014**, *53*, 365–368; *Angew. Chem.* **2014**, *126*, 373–376; e) V. K. Praveen, C. Ranjith, E. Bandini, A. Ajayaghosh, N. Armaroli, *Chem. Soc. Rev.* **2014**, *43*, 4222–4242.

[4] a) D. J. Abdallah, R. G. Weiss, *Adv. Mater.* **2000**, *12*, 1237–1247; b) T. Ishi, S. Shinkai, *Top. Curr. Chem.* **2005**, *258*, 119–160; c) V. K. Praveen, S. S. Babu, C. Vijayakumar, R. Varghese, A. Ajayaghosh, *Bull. Chem. Soc. Jpn.* **2008**, *81*, 1196–1211; d) S. Banerjee, R. K. Das, U. Maitra, *J. Mater. Chem.* **2009**, *19*, 6649–6687; e) J.-L. Li, X.-Y. Liu, *Adv. Funct. Mater.* **2010**, *20*, 3196–3216; f) A. Dawn, T. Shiraki, S. Haraguchi, S.-i. Tamaru, S. Shinkai, *Chem. Asian J.* **2011**, *6*, 266–282; g) K. K. Kartha, R. D. Mukhopadhyay, A. Ajayaghosh, *Chimia* **2013**, *67*, 51–63.

[5] a) T. F. A. De Greef, M. M. J. Smulders, M. Wolffs, A. P. H. J. Schenning, R. P. Sijbesma, E. W. Meijer, *Chem. Rev.* **2009**, *109*, 5687–5754; b) Z. Chen, A. Lohr, C. R. Saha-Möller, F. Würthner, *Chem. Soc. Rev.* **2009**, *38*, 564–584; c) C. Kulkarni, S. Balasubramanian, S. J. George, *ChemPhysChem* **2013**, *14*, 661–673; d) P. A. Korevaar, T. F. A. de Greef, E. W. Meijer, *Chem. Mater.* **2014**, *26*, 576–586; e) C. Rest, R. Kandanelli, G. Fernández, *Chem. Soc. Rev.* **2015**, *44*, 2543–2572.

[6] a) F. García, L. Sánchez, *J. Am. Chem. Soc.* **2012**, *134*, 734–742; b) J. M. Malicka, A. Sandeep, F. Monti, E. Bandini, M. Gazzano, C. Ranjith, V. K. Praveen, A. Ajayaghosh, N. Armaroli, *Chem. Eur. J.* **2013**, *19*, 12991–13001; c) S. Ogi, K. Sugiyasu, S. Manna, S. Samitsu, M. Takeuchi, *Nat. Chem.* **2014**, *6*, 188–195; d) J. Kang, D. Miyajima, T. Mori, Y. Inoue, Y. Itoh, T. Aida, *Science* **2015**, *347*, 646–651; e) S. Ogi, V. Stepanenko, K. Sugiyasu, M. Takeuchi, F. Würthner, *J. Am. Chem. Soc.* **2015**, *137*, 3300–3307.

[7] a) *The Amide Linkage: Structural Significance in Chemistry, Biochemistry and Materials Science* (Eds.: A. Greenberg, C. M. Breneman, J. F. Liebman), Wiley, NJ, **2003**; b) F. Fages, F. Vögtle, M. Žinić, *Top. Curr. Chem.* **2005**, *256*, 77–131; c) M. R. Rao, S.-S. Sun, *Langmuir* **2013**, *29*, 15146–15158.

[8] a) X. Yang, G. Zhang, D. Zhang, *J. Mater. Chem.* **2012**, *22*, 38–50; b) X. Yan, F. Wang, B. Zheng, F. Huang, *Chem. Soc. Rev.* **2012**, *41*, 6042–6065; c) M. D. Segarra-Maset, V. J. Nebot, J. F. Miravet, B. Escuder, *Chem. Soc. Rev.* **2013**, *42*, 7086–7098; d) X. Yu, L. Chen, M. Zhang, T. Yi, *Chem. Soc. Rev.* **2014**, *43*, 5346–5371; e) S. Mahesh, R. Thirumalai, S. Yagai, A. Kita-

mura, A. Ajayaghosh, *Chem. Commun.* **2009**, 5984 – 5986; f) S. Yagai, H. Aonuma, Y. Kikkawa, S. Kubota, T. Karatsu, A. Kitamura, S. Mahesh, A. Ajayaghosh, *Chem. Eur. J.* **2010**, *16*, 8652 – 8661.

[9] a) B. Xing, M.-F. Choi, B. Xu, *Chem. Eur. J.* **2002**, *8*, 5028 – 5032; b) S. Arai, K. Imazu, S. Kusuda, I. Yoshihama, M. Tonegawa, Y. Nishimura, K.-i. Kitahara, S. Oishi, T. Takemura, *Chem. Lett.* **2006**, *35*, 634 – 635; c) K. Yabuuchi, T. Kato, *Mol. Cryst. Liq. Cryst.* **2005**, *441*, 261 – 273; d) H.-J. Kim, J.-H. Lee, M. Lee, *Angew. Chem. Int. Ed.* **2005**, *44*, 5810 – 5814; *Angew. Chem.* **2005**, *117*, 5960 – 5964; e) H.-J. Kim, E. Lee, H.-S. Park, M. Lee, *J. Am. Chem. Soc.* **2007**, *129*, 10994 – 10995; f) Y.-R. Liu, L. He, J. Zhang, X. Wang, C.-Y. Su, *Chem. Mater.* **2009**, *21*, 557 – 563; g) S. Shin, S. Lim, Y. Kim, T. Kim, T.-L. Choi, M. Lee, *J. Am. Chem. Soc.* **2013**, *135*, 2156 – 2159; h) S. Bhattacharjee, S. K. Samanta, P. Moitra, K. Pramoda, R. Kumar, S. Bhattacharya, C. N. R. Rao, *Chem. Eur. J.* **2015**, *21*, 5467 – 5476.

[10] a) H.-C. Lin, C.-M. Tsai, G.-H. Huang, Y.-T. Tao, *Macromolecules* **2006**, *39*, 557 – 568; b) J. Seo, J. W. Chung, E.-H. Jo, S. Y. Park, *Chem. Commun.* **2008**, 2794 – 2796; c) P. Duan, X. Zhu, M. Liu, *Chem. Commun.* **2011**, *47*, 5569; d) Y. J. Adhia, T. H. Schloemer, M. T. Perez, A. J. McNeil, *Soft Matter* **2012**, *8*, 430 – 434; e) S. K. Samanta, S. Bhattacharya, *Chem. Commun.* **2013**, *49*, 1425 – 1427; f) S. Bhattacharjee, S. Bhattacharya, *Chem. Commun.* **2015**, *51*, 6765 – 6768; g) S. Bhattacharjee, S. Bhattacharya, *Chem. Commun.* **2015**, *51*, 7019 – 7022.

[11] For pyridyl-urea based systems, see: a) D. K. Kumar, D. A. Jose, A. Das, P. Dastidar, *Chem. Commun.* **2005**, 4059 – 4061; b) L. S. Reddy, S. Basavoju, V. R. Vangala, A. Nangia, *Cryst. Growth Des.* **2006**, *6*, 161 – 173; c) R. Custelcean, V. Sellin, B. A. Moyer, *Chem. Commun.* **2007**, 1541 – 1543; d) N. N. Adarsh, D. K. Kumar, P. Dastidar, *Tetrahedron* **2007**, *63*, 7386 – 7396; e) P. Byrne, D. R. Turner, G. O. Lloyd, N. Clarke, J. W. Steed, *Cryst. Growth Des.* **2008**, *8*, 3335 – 3344; f) M.-O. M. Piepenbrock, N. Clarke, J. W. Steed, *Langmuir* **2009**, *25*, 8451 – 8456; g) P. Byrne, G. O. Lloyd, L. Applegarth, K. M. Anderson, N. Clarke, J. W. Steed, *New J. Chem.* **2010**, *34*, 2261 – 2274; h) M.-O. M. Piepenbrock, N. Clarke, J. W. Steed, *Soft Matter* **2010**, *6*, 3541 – 3547; i) L. Meazza, J. A. Foster, K. Fucke, P. Metrangolo, G. Resnati, J. W. Steed, *Nat. Chem.* **2013**, *5*, 42 – 47.

[12] a) A. Ajayaghosh, S. J. George, *J. Am. Chem. Soc.* **2001**, *123*, 5148 – 5149; b) S. J. George, A. Ajayaghosh, *Chem. Eur. J.* **2005**, *11*, 3217 – 3227; c) A. Ajayaghosh, V. K. Praveen, *Acc. Chem. Res.* **2007**, *40*, 644 – 656; d) A. Ajayaghosh, C. Vijayakumar, R. Varghese, S. J. George, *Angew. Chem. Int. Ed.* **2006**, *45*, 456 – 460; *Angew. Chem.* **2006**, *118*, 470 – 474; e) V. K. Praveen, S. J. George, A. Ajayaghosh, *Macromol. Symp.* **2006**, *241*, 1 – 8; f) A. Ajayaghosh, C. Vijayakumar, V. K. Praveen, S. S. Babu, R. Varghese, *J. Am. Chem. Soc.* **2006**, *128*, 7174 – 7175.

[13] a) R. Varghese, S. J. George, A. Ajayaghosh, *Chem. Commun.* **2005**, 593 – 595; b) A. Ajayaghosh, V. K. Praveen, S. Srinivasan, R. Varghese, *Adv. Mater.* **2007**, *19*, 411 – 415; c) S. S. Babu, V. K. Praveen, S. Prasanthkumar, A. Ajayaghosh, *Chem. Eur. J.* **2008**, *14*, 9577 – 9584; d) S. S. Babu, V. K. Praveen, A. Ajayaghosh, *Macromol. Symp.* **2008**, *273*, 25 – 32; e) V. R. R. Kumar, V. Sajini, T. S. Sreeprasad, V. K. Praveen, A. Ajayaghosh, T. Pradeep, *Chem. Asian J.* **2009**, *4*, 840 – 848; f) C. Vijayakumar, V. K. Praveen, K. K. Kartha, A. Ajayaghosh, *Phys. Chem. Chem. Phys.* **2011**, *13*, 4942 – 4949; g) A. Gopal, R. Varghese, A. Ajayaghosh, *Chem. Asian J.* **2012**, *7*, 2061 – 2067; h) S. S. Babu, V. K. Praveen, K. K. Kartha, S. Mahesh, A. Ajayaghosh, *Chem. Asian J.* **2014**, *9*, 1830 – 1840.

[14] a) S. S. Babu, S. Mahesh, K. K. Kartha, A. Ajayaghosh, *Chem. Asian J.* **2009**, *4*, 824 – 829; b) D. Dasgupta, S. Srinivasan, C. Rochas, A. Thierry, A. Schröder, A. Ajayaghosh, J. M. Guenet, *Soft Matter* **2011**, *7*, 2797 – 2804; c) D. Dasgupta, S. Srinivasan, C. Rochas, A. Ajayaghosh, J.-M. Guenet, *Soft Matter* **2011**, *7*, 9311 – 9315; d) D. Dasgupta, S. Srinivasan, A. Ajayaghosh, J. M. Guenet, *Macromol. Symp.* **2011**, *303*, 134 – 140; e) D. Dasgupta, A. Thierry, C. Rochas, A. Ajayaghosh, J. M. Guenet, *Soft Matter* **2012**, *8*, 8714 – 8721.

[15] a) J. F. Hulvat, M. Sofos, K. Tajima, S. I. Stupp, *J. Am. Chem. Soc.* **2005**, *127*, 366 – 372; b) S. Yagai, S. Kubota, T. Iwashima, K. Kishikawa, T. Nakanishi, T. Karatsu, A. Kitamura, *Chem. Eur. J.* **2008**, *14*, 5246 – 5257; c) S. K. Samanta, A. Pal, S. Bhattacharya, *Langmuir* **2009**, *25*, 8567 – 8578; d) P. Xue, R. Lu, X. Yang, L. Zhao, D. Xu, Y. Liu, H. Zhang, H. Nomoto, M. Takafuji, H. Ihara, *Chem. Eur. J.* **2009**, *15*, 9824 – 9835; e) J. Hou, X. Wu, Y.-J. Li, *Supramol. Chem.* **2011**, *23*, 533 – 538; f) M. Mba, A. Moretto, L. Armelao, M. Crisma, C. Toniolo, M. Maggini, *Chem. Eur. J.* **2011**, *17*, 2044 – 2047; g) S. Yagai, K. Ishiwatari, X. Lin, T. Karatsu, A. Kitamura, S. Uemura, *Chem. Eur. J.* **2013**, *19*, 6971 – 6975; h) B. D. Wall, A. E. Zacca, A. M. Sanders, W. L. Wilson, A. L. Ferguson, J. D. Tovar, *Langmuir* **2014**, *30*, 5946 – 5956; i) C. Yao, Q. Lu, X. Wang, F. Wang, *J. Phys. Chem. B* **2014**, *118*, 4661 – 4668.

[16] a) B. Wang, M. R. Wasielewski, *J. Am. Chem. Soc.* **1997**, *119*, 12 – 21; b) V. K. Praveen, S. J. George, R. Varghese, C. Vijayakumar, A. Ajayaghosh, *J. Am. Chem. Soc.* **2006**, *128*, 7542 – 7550.

[17] a) J. M. J. Paulusse, R. P. Sijbesma, *Angew. Chem. Int. Ed.* **2006**, *45*, 2334 – 2337; *Angew. Chem.* **2006**, *118*, 2392 – 2396; b) D. Bardelang, *Soft Matter* **2009**, *5*, 1969 – 1971; c) G. Cravotto, P. Cintas, *Chem. Soc. Rev.* **2009**, *38*, 2684 – 2697.

[18] a) A. R. Hirst, D. K. Smith, *Chem. Eur. J.* **2005**, *11*, 5496 – 5508; b) J. Raeburn, D. J. Adams, *Chem. Commun.* **2015**, *51*, 5170 – 5180.

[19] a) W. Herrebout, K. Clou, H. O. Desseyn, N. Blaton, *Spectrochim. Acta Part A* **2003**, *59*, 47 – 59; b) E. Jahnke, J. Weiss, S. Neuhaus, T. N. Hoheisel, H. Frauenrath, *Chem. Eur. J.* **2009**, *15*, 388 – 404; c) R. Abbel, R. van der Weegen, W. Pisula, M. Surin, P. Leclère, R. Lazzaroni, E. W. Meijer, A. P. H. J. Schenning, *Chem. Eur. J.* **2009**, *15*, 9737 – 9746; d) Y. Sagara, S. Yamane, T. Mutai, K. Araki, T. Kato, *Adv. Funct. Mater.* **2009**, *19*, 1869 – 1875; e) K. Isozaki, Y. Haga, K. Ogata, T. Naota, H. Takaya, *Dalton Trans.* **2013**, *42*, 15953 – 15966.

[20] a) F. D. Lewis, J.-S. Yang, C. L. Stern, *J. Am. Chem. Soc.* **1996**, *118*, 2772 – 2773; b) F. D. Lewis, J.-S. Yang, C. L. Stern, *J. Am. Chem. Soc.* **1996**, *118*, 12029 – 12037; c) F. D. Lewis, J.-S. Yang, *J. Phys. Chem. B* **1997**, *101*, 1775 – 1781.

Manuscript received: April 1, 2015
Accepted Article published: April 30, 2015
Final Article published: June 12, 2015